

## Effects of Divalent Cations on the E-4031-Sensitive Repolarization Current, $I_{Kr}$ , in Rabbit Ventricular Myocytes

Tyna Paquette,\* John R. Clay,# Azieb Ogbaghebriel,\* and Alvin Shrier\*

\*Department of Physiology, McGill University, Montréal, Québec H3G 1Y6, Canada, and #Laboratory of Neurophysiology, National Institute for Neurological Disorders and Stroke, National Institutes of Health, Bethesda, Maryland 20892 USA

**ABSTRACT** The effects of divalent cations on the E-4031-sensitive repolarization current ( $I_{Kr}$ ) were studied in single ventricular myocytes isolated from rabbit hearts. One group of divalent cations ( $Cd^{2+}$ ,  $Ni^{2+}$ ,  $Co^{2+}$ , and  $Mn^{2+}$ ) produced a rightward shift of the  $I_{Kr}$  activation curve along the voltage axis, increased the maximum  $I_{Kr}$  amplitude (i.e., relieved the apparent inward rectification of the channel), and accelerated  $I_{Kr}$  tail current kinetics. Another group ( $Ca^{2+}$ ,  $Mg^{2+}$  and  $Sr^{2+}$ ) had relatively little effect on  $I_{Kr}$ . The only divalent cation that blocked  $I_{Kr}$  was  $Zn^{2+}$  (0.1–1 mM). Under steady-state conditions,  $Ba^{2+}$  caused a substantial block of  $I_{Kr}$ , as previously reported. However, block by  $Ba^{2+}$  was time dependent, which precluded a study of  $Ba^{2+}$  effects on  $I_{Kr}$ . We conclude that the various effects of the divalent cations can be attributed to interactions with distinct sites associated with the rectification and/or inactivation mechanism of the channel.

### INTRODUCTION

Potassium channels play an important role in the maintenance of resting potential and in determining the action potential duration of cardiac cells. For example, the relatively negative resting potential of ventricular myocardial cells is attributable to the background potassium ion current,  $I_{K1}$ , which also contributes to the late phase of repolarization of the action potential (Giles and Imaizumi, 1988; Shimoni et al., 1992). The  $I_{K1}$  channel is open at the resting potential, but strongly rectifies with depolarization, so that it contributes essentially no current for potentials positive to  $\sim -20$  mV. The mechanism underlying  $I_{K1}$  rectification is thought to involve voltage-dependent block of the channel pore by intracellular  $Mg^{2+}$  (Matsuda et al., 1987; Vandenberg, 1987) and/or the polyamines spermine and spermidine (Ficker et al., 1994). A second inwardly rectifying current in cardiac muscle, the E-4031-sensitive current,  $I_{Kr}$ , also plays an important role in repolarization (Noble and Tsien, 1969; Shrier and Clay, 1986; Sanguinetti and Jurkiewicz, 1990a). This component is rapidly activated during the plateau phase of the action potential, but contributes relatively little current until the membrane potential is repolarized below 0 mV. The mechanism for this effect was originally attributed to inward rectification of the  $I_{Kr}$  channel, similar to that for  $I_{K1}$  (Shrier and Clay, 1986). However, recent work on heterologous expression of the HERG channel has clearly demonstrated that rectification of  $I_{Kr}$  is, instead, attributable to rapid, voltage-dependent inactivation similar to that of other kinds of  $K^+$  channels (Smith et al., 1996; Spector et al., 1996).

Divalent cations have been one of the classical tools used to probe potassium ion channel gating and permeation (Hille, 1992). For example, Standen and Stanfield (1978) found a time- and voltage-dependent block of  $I_{K1}$  in skeletal muscle fibers by  $Ba^{2+}$  and  $Sr^{2+}$ , which they attributed to competition between  $Ba^{2+}$  and  $Sr^{2+}$  with  $K^+$  for a site deep within the aqueous pore of the  $I_{K1}$  channel. A similar result was reported for  $Sr^{2+}$  with the  $I_{K1}$  channel in guinea pig ventricular myocytes by Shioya et al. (1993). Divalent cations have also been shown to block the delayed rectifier potassium ion current in squid giant axons (Eaton and Brodwick, 1980; Armstrong and Taylor, 1980; Clay, 1995). In guinea pig cardiac cells,  $I_{Kr}$  and  $I_{Ks}$  have been reported to have differing sensitivities to divalent cations (Sanguinetti and Jurkiewicz, 1990a,b). However, the effects of divalent cations on  $I_{Kr}$  have not been elucidated. Follmer et al. (1992) found that the addition of 0.2 mM  $Cd^{2+}$  to the extracellular solution, a condition that has often been used to block  $I_{Ca}$ , actually increased  $I_{Kr}$  amplitude in cat ventricular myocytes. A similar result has recently been reported in guinea-pig ventricular myocytes by Daleau et al. (1997). We have expanded upon this work, using rabbit ventricular myocytes and various other divalent cations in addition to  $Cd^{2+}$ . We found that  $Ni^{2+}$ ,  $Mn^{2+}$ , and  $Co^{2+}$  all produced potentiation of  $I_{Kr}$  similar to the  $Cd^{2+}$  result, which we have attributed to the alteration of  $I_{Kr}$  inactivation. In contrast,  $Zn^{2+}$  (0.1–1 mM) blocked  $I_{Kr}$ . The effects of  $Ba^{2+}$  on  $I_{Kr}$  could not be readily characterized because of a  $Ba^{2+}$ -induced time- and voltage-dependent current attributed to an interaction between  $Ba^{2+}$  and the  $I_{K1}$  channel, as reported previously (Standen and Stanfield, 1978).

### MATERIALS AND METHODS

#### Isolation of ventricular myocytes

Single ventricular cells from rabbit hearts were prepared by using a modification of techniques described by Mitra and Morad (1985). New Zealand white rabbits weighing 1.6–2.5 kg were anesthetized with a

Received for publication 3 June 1997 and in final form 9 December 1997.

Address reprint requests to Dr. Alvin Shrier, Physiology Department, McGill University, 3655 Drummond Street, Montréal Québec H3G 1Y6, Canada. Tel.: 514-398-4318; Fax: 514-398-7452; E-mail: ashrier@physio.mcgill.ca.

© 1998 by the Biophysical Society

0006-3495/98/03/1278/08 \$2.00

combination of ketamine (70 mg/kg) and xylazine (10 mg/kg), and exsanguinated via the carotid artery. The hearts were excised, mounted on a Langendorff reperfusion apparatus, and perfused at 37°C with normal Tyrode's solution (see below) for 5 min followed by an additional 10 min of perfusion with nominally  $Ca^{2+}$ -free Tyrode's solution. The hearts were then perfused for 5–10 min with  $Ca^{2+}$ -free Tyrode's solution containing collagenase (type IA 33 units/ml; Sigma Chemical Co., St. Louis, MO), followed by an additional 5–10 min of perfusion with a solution containing collagenase and protease (type XIV, 0.14 units/ml; Sigma Chemical Co.). Pieces of the ventricle were cut and placed in a K-B solution (Isenberg and Klockner, 1982) and agitated gently. The resulting single-cell suspension was stored in K-B solution at room temperature. Cells were used for electrophysiological recordings within 1–8 h.

## Solutions

The Tyrode's solution used in the cell isolation procedure contained (in mM) 121 NaCl, 5 KCl, 15  $NaHCO_3$ , 1  $Na_2HPO_4$ , 2.8 sodium acetate, 1  $MgCl_2$ , 2.2  $CaCl_2$ , and 5.5 glucose, gassed with 95%  $O_2$ /5%  $CO_2$  mixture. For the  $Ca^{2+}$ -free Tyrode's solution, the 2.2 mM  $CaCl_2$  was omitted. The K-B solution was a modification from Isenberg and Klockner, (1982) which contained (in mM) 85 KCl, 30  $K_2HPO_4$ , 5  $MgSO_4$ , 5  $K_2ATP$ , 5 sodium pyruvate, 5  $\beta$ -OH-butyric acid, 5 creatine, 20 taurine, 20 glucose, 11 succinic acid, 0.62 polyvinylpyrrolidone, and 0.5 EGTA. The pH was adjusted to 7.2 with KOH. The extracellular solution used during electrophysiological recordings contained (in mM) 121 NaCl, 5 KCl, 2.8 sodium acetate, 1  $MgCl_2$ , 2.2  $CaCl_2$ , 10 HEPES, and 10 glucose with the pH adjusted to 7.4 with NaOH. The extracellular solution was continuously gassed with 100%  $O_2$ . The solution in the recording pipette contained (in mM) 140 KCl, 5 ATP disodium salt, 5 creatine phosphate disodium salt, 1  $MgCl_2$ , 5 HEPES, 5 EGTA, and 1.54  $CaCl_2$  with the pH adjusted to 7.2 with KOH (pCa 7.2; pMg 4.2). The calcium current was completely blocked with nifedipine (5–10  $\mu$ M) (Sigma Chemical Co.). E-4031 was kindly provided by Eisai Co. (Tsukuba Research Laboratories, Japan). Various concentrations (10  $\mu$ M to 5 mM) of divalent cations ( $CdCl_2$ ,  $ZnCl_2$ ,  $BaCl_2$ ,  $NiCl_2$ ,  $CoCl_2$ ,  $CaCl_2$ ,  $MnCl_2$ ,  $SrCl_2$ , and  $MgCl_2$ ) were added to the extracellular solution from stock solutions of 1 M concentration. In a few experiments with 5 mM  $CdCl_2$ , the NaCl concentration was reduced by 10 mM to keep the ionic strength of the extracellular solution constant.

## Electrical recording and data analysis

The whole-cell patch-clamp technique was used to record membrane currents in these experiments. Ventricular cells were placed in a chamber mounted on the stage of an inverted microscope (Zeiss IM35, Oberkochen, Germany) and allowed to settle for ~5–10 min. The cells were continuously superfused with extracellular solution (see above) at 33–35°C. Rod-shaped myocytes with clear striations were selected for electrical recordings using an Axopatch amplifier (Axopatch-1D; Axon Instruments Corp., Foster City, CA). The pipette tip resistance was 2–4 M $\Omega$ . The input capacitance of the cells was in the 50–95-pF range. Voltage clamp pulses were delivered from a custom-designed software package (Alembic Software Co., Montréal, Canada) implemented on a personal computer equipped with an analog-to-digital card (Omega Corp., Stanford, CT). The

holding potential used throughout was  $-40$  mV, which effectively inactivates both the sodium ion current,  $I_{Na}$ , and the transient outward current,  $I_{to}$  (Ogbaghebiel and Shrier, 1994). Membrane currents and voltages were filtered at 10 kHz, digitized at 22 kHz via a pulse code modulation unit (Neurocorder DR-390; NeuroData Corp., New York, NY), and recorded on a Betamax VCR (SL-HF 450; Sony Corp., New York, NY). Currents were analyzed off-line at 5 kHz and digitized by a 12-bit analog-to-digital converter at 10 kHz.

## RESULTS

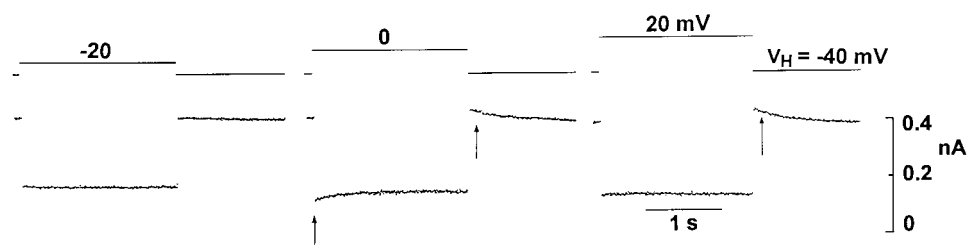
### Properties of $I_{Kr}$ in control conditions

Representative recordings of membrane currents obtained in this study are illustrated in Fig. 1. The steady-state holding current at  $-40$  mV was 0.39 nA, which was attributable to  $I_{K1}$  (Carmeliet, 1993). Moreover,  $-40$  mV lies on the negative slope region of the  $I_{K1}$  current-voltage relation, as shown by the instantaneous current jumps in the inward direction in all steps. (The steady state at the end of 0 and  $+20$  mV steps is probably attributable to a "leak" current component.) With increasing depolarizations, a time-dependent outward going current,  $I_{Kr}$ , was elicited as indicated by the arrows in Fig. 1. These results are shown in more detail in Fig. 2, in which the steady-state current has been subtracted and the current scale amplified. (The top four records in Fig. 2 were taken from the same preparation as in Fig. 1.) These records indicate that the threshold for activation of  $I_{Kr}$  was between  $-20$  and  $-10$  mV and the conductance saturated at  $\sim +10$  to  $+20$  mV. Time-dependent current during the voltage steps themselves was evident at  $\sim -20$  to  $-10$  mV, and became smaller with increasing depolarizations, so that it was essentially nil at  $+20$  mV, as expected for  $I_{Kr}$  (Sanguinetti and Jurkiewicz, 1990a; Clay et al., 1995). The  $I_{Kr}$  component was completely blocked by E-4031 (1  $\mu$ M), as shown in Fig. 2. A complete biophysical analysis of these results is given in Clay et al. (1995).

### Effect of divalent cations on $I_{Kr}$

Follmer et al. (1992) previously reported that  $Cd^{2+}$ , at a concentration used to block the calcium ion current (0.2 mM), modified the kinetic and ion transfer properties of  $I_{Kr}$ . We have expanded upon their work by using a larger concentration of  $Cd^{2+}$  (5 mM), as well as testing the effects of other divalent cations. Fig. 3 illustrates our results with 5

FIGURE 1 Control recordings of membrane current from a rabbit ventricular myocyte. These results were obtained by stepping the membrane potential to the voltages indicated for 2 s, followed by a return to the holding level ( $-40$  mV). The holding current was 0.39 nA.



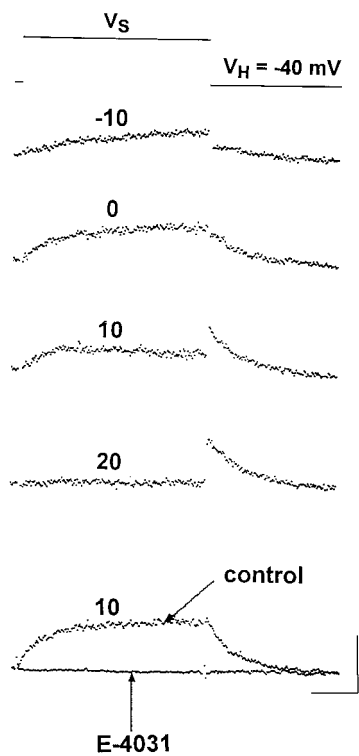
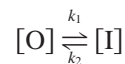


FIGURE 2 The time-dependent currents ( $I_{Kr}$ ). The top four recordings were obtained from the corresponding results of the preparation in Fig. 1 with the steady-state current subtracted. The step potential ( $V_S$ ) is indicated above each recording. The bottom panel illustrates the blocking effect of 1  $\mu$ M E-4031 on  $I_{Kr}$ . These results were taken from a preparation different from that of the other recordings shown here. Calibrations are 0.5 s and 0.05 nA.

mM  $Cd^{2+}$ . Cadmium shifted the activation curve to more positive potentials (Fig. 3 A) and increased the rate of  $I_{Kr}$  deactivation (Fig. 3 B, *inset*), which is similar to the effects of divalent cations on voltage-gated conductances in nerve axon (Frankenhaeuser and Hodgkin, 1957; Gilly and Armstrong, 1982a,b). Moreover, the amplitude of  $I_{Kr}$  tail current was significantly increased by 5 mM  $Cd^{2+}$ , especially at  $-20$  mV (Fig. 3 B, and records to the left of Fig. 3 A). The latter effect appeared to be entirely attributable to  $I_{Kr}$ , inasmuch as the tail currents with 5 mM  $Cd^{2+}$  were completely blocked by 1  $\mu$ M E-4031 (Fig. 3, *inset*). The activation curves in Fig. 3 A were fit with the Boltzmann relation,  $f_o(1 + \exp(-(V - V_{1/2})/V_S))^{-1}$ , where  $V_{1/2} = 12$  or  $36$  mV;  $V_S = 9.1$  or  $10.0$  mV; and  $f_o = 1$  or  $1.75$ , respectively, for control and 5 mM  $Cd^{2+}$  conditions. The fit to the  $Cd^{2+}$  results is also shown with  $f_o = 1$  (Fig. 3 A, *dashed curve*) to better illustrate the voltage shift. The results in Fig. 3 B were obtained with a 1-s prepulse to  $+60$  mV to fully activate the  $I_{Kr}$  conductance in both control and 5 mM  $Cd^{2+}$  conditions, followed by a step to various potentials of less than  $+60$  mV. The amplitudes of the current obtained by the second step in this protocol are shown in Fig. 3 B for control and test conditions. All of these results have been normalized to the maximum outward current in control, which occurred

at  $\sim -40$  mV. We previously modeled the rectification of the fully activated current-voltage relation for  $I_{Kr}$  by assuming that a blocking particle (either membrane bound or in the cytoplasm) moved some distance into the channel with membrane depolarization, thereby reducing outward current in a voltage-dependent manner without significantly altering inward current (Clay et al., 1995). Alternatively, the effect can also be modeled by a rapid, voltage-gated inactivation process that has been shown to underlie the apparent rectification of  $I_{Kr}$  (Smith et al., 1996; Spector et al., 1996). That is, the  $I_{Kr}$  channel is assumed to make transitions between its open and inactivated states, i.e.,



so that the probability that the open state is occupied ( $p_o$ ) immediately after a prepulse to  $+60$  mV is  $p_o = (1 + k_1/k_2)^{-1}$ , where  $k_1$  and  $k_2$  are functions of membrane potential. Consequently, the fully activated current-voltage relation for  $I_{Kr}$  is given by  $g(V - E_{Kr})/(1 + k_1/k_2)$ , where  $g$  is its limiting slope conductance ( $V \rightarrow -\infty$ ) and  $E_{Kr}$  is its reversal potential. This equation was fit, by eye, to the results in Fig. 3 B by using  $k_1/k_2 = 6 \exp(0.05V)$  and  $E_{Kr} = -70$  mV. In other words, the experimentally observed rectification of  $I_{Kr}$  is sufficient to determine the ratio of  $k_1$  and  $k_2$ . Direct measurements of the inactivation kinetics themselves, which we have been unable to carry out because they are so fast (even at room temperature), would be required to determine  $k_1$  and  $k_2$  separately. We have assumed that  $Cd^{2+}$  alters these kinetics by binding to the inactivation gate, so that the rate constant  $k_1$  is reduced, i.e.,  $k_1 = k_1^o(1 + [Cd^{2+}]/K_D)^{-1}$ , where  $[Cd^{2+}]$  is the cadmium concentration, and  $K_D$  is the dissociation constant for the binding of  $Cd^{2+}$  to the gate. For the  $Cd^{2+}$  results in Fig. 3 B, we used  $k_1/k_2 = 0.8 \exp(0.085V)$ , which is consistent with  $K_D = 0.74$  mM. (We have not yet determined the significance of the slight change in electrical distance of the inactivation gating in the presence of  $Cd^{2+}$ , which this result implies.) This analysis illustrates one way in which  $I_{Kr}$  amplitude can be increased by  $Cd^{2+}$ . Other models of the  $Cd^{2+}$  effect may be equally likely (see Discussion).

As shown in Table 1,  $Ni^{2+}$ ,  $Co^{2+}$ , and  $Mn^{2+}$  all had effects similar to those of  $Cd^{2+}$  in terms of the change in rectification (increase in maximum outward current), with  $Cd^{2+}$  being more potent than any other divalent cation ( $Cd^{2+} > Ni^{2+} \approx Co^{2+} \approx Mn^{2+}$ ), whereas  $Ni^{2+}$  produced approximately the same shift in the  $I_{Kr}$  activation curve as  $Cd^{2+}$ , with  $Co^{2+}$  and  $Mn^{2+}$  being considerably less potent ( $Cd^{2+} \approx Ni^{2+} > Co^{2+} \approx Mn^{2+}$ ). The fully activated current-voltage relation in control (2 mM  $Ca^{2+}$ ) was essentially unchanged with 5 mM  $Ca^{2+}$  (results not shown). Magnesium and strontium had a similar lack of effect on  $I_{Kr}$ . In these experiments we simply added divalent cations to the extracellular solution, thereby slightly increasing ionic strength. We confirmed that the increase in ionic strength was not a contributing factor in a series of control

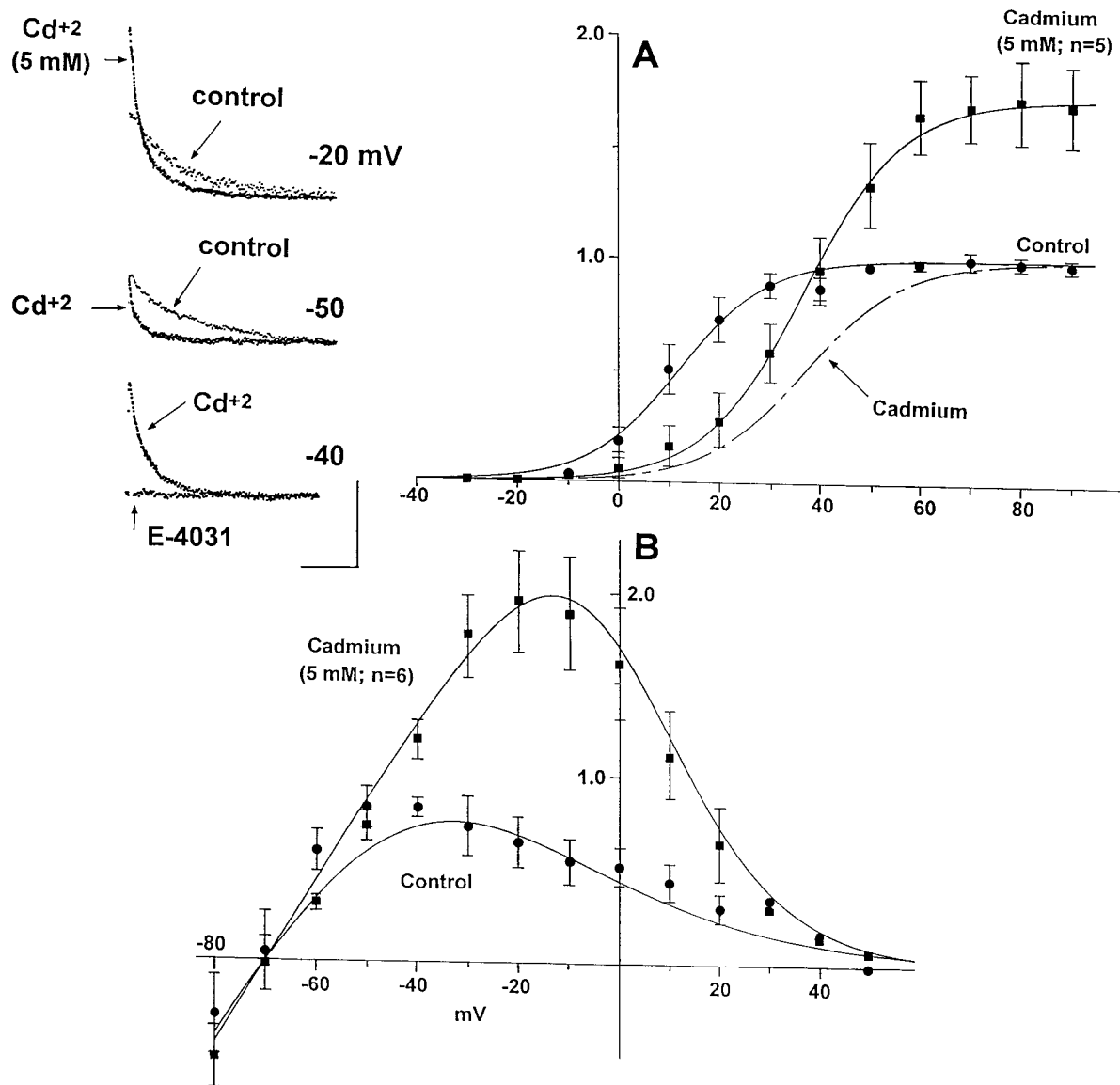


FIGURE 3 Effects of cadmium on activation and current-voltage relation of  $I_{Kr}$ . (A) Activation curve in control (●) and in the presence of 5 mM  $Cd^{2+}$  in the extracellular solution (■). These results were obtained from tail current amplitudes at the holding potentials ( $-40$  mV) after 2-s duration voltage steps to the potential on the abscissa. Each symbol represents the  $\bar{x} \pm SD$  from five different cells. All results were normalized by the maximum tail current obtained in the control. The test results illustrate the significant increase in  $I_{Kr}$  induced by  $Cd^{2+}$  and a few other divalent cations (Table 1). This effect is shown explicitly by the records in the inset alongside A. The results in A also illustrate the voltage shift of  $I_{Kr}$  activation, which is further described by the theoretical curves in A. The curve describing the control results is a best fit (least-squares minimization) of the Boltzmann relation,  $(1 + \exp(-(V - V_{1/2})/V_S))^{-1}$ , where  $V_{1/2} = 12$  mV and the slope factor  $V_S = 9.1$  mV. The curve describing the  $Cd^{2+}$  results represents  $f_o(1 + \exp(-(V - V_{1/2})/V_S))^{-1}$ , where  $f_o = 1.75$ ,  $V_{1/2} = 36$  mV, and  $V_S = 10.0$  mV. This result is also shown with  $f_o = 1$  (dashed curve) to better illustrate the voltage shift of the activation curve. (B) Effect of 5 mM  $Cd^{2+}$  on the fully activated current-voltage ( $I$ - $V$ ) relation of  $I_{Kr}$  ( $\bar{x} \pm SD$ ;  $n = 6$ ). All results were normalized to the maximum outward current obtained in the control. These results correspond to amplitudes of the time-dependent current elicited by a voltage step to the potentials indicated on the abscissa after a 1-s-duration prepulse to  $+60$  mV. The curve describing the control results (●) is given by  $0.043(V + 70)/(1 + 6 \exp(0.05V))$ . The curve describing the  $Cd^{2+}$  results (■) is given by  $0.043(V + 70)/(1 + 0.8 \exp(0.085V))$ . The theoretical basis for these relationships is given in the Results. (Inset) Control and test results are shown superimposed to the right for  $-20$  and  $-50$  mV. Block of the time-dependent current with 5 mM  $Cd^{2+}$  by 1  $\mu$ M E-4031 is shown by the records in the bottom panel of the inset. Calibrations are 0.5 s and 0.1 nA.

experiments in which ionic strength was maintained constant (see Materials and Methods). In particular, the voltage shift with 5 mM  $Cd^{2+}$  was  $+23.5$  mV (mean from two experiments, 22 and 25 mV, respectively), which is similar to the results obtained when ionic strength was not kept constant.

The only divalent cation that blocked  $I_{Kr}$  was  $Zn^{2+}$ , as shown in Fig. 4 A. The  $I_{Kr}$  amplitude was reduced by  $\sim 20\%$  with 0.1 mM  $Zn^{2+}$  and by  $\sim 75\%$  with 1 mM  $Zn^{2+}$ . The records in Fig. 4 B illustrate a preparation in which  $I_{Kr}$  was completely blocked by 1 mM  $Zn^{2+}$ , as indicated by the tail currents after a voltage step to  $+20$  mV. These results also

**TABLE 1** Effects of divalent cations on  $I_{Kr}$ 

Divalent Cation 5mM	Shift of $I_{Kr}$ Activation (mV)	Removal of $I_{Kr}$ Rectification <sup>#</sup>
Cd <sup>2+</sup>	+26.6 ± 3.6*	2.32 ± 0.43
Ni <sup>2+</sup>	+23.5 ± 4.6	1.45 ± 0.15
Co <sup>2+</sup>	+14.7 ± 3.7	1.41 ± 0.14
Mn <sup>2+</sup>	+11.0 ± 3.5	1.32 ± 0.08
Sr <sup>2+</sup>	+1.8 ± 0.6	—
Ca <sup>2+</sup>	+3.1 ± 1.9	—
Mg <sup>2+</sup>	-3.7 ± 2.9	—

\* $\bar{x} \pm$  S.D.,  $n = 3-7$ .

<sup>#</sup>Peak  $I_{Kr}$  in 5 mM divalent cation/peak  $I_{Kr}$  control.

Sequence of effects of divalent cations: increase of  $I_{Kr}$  amplitude: Cd<sup>2+</sup> >> Ni<sup>2+</sup> ≈ Co<sup>2+</sup> ≈ Mn<sup>2+</sup> > Ca<sup>2+</sup> ≈ Sr<sup>2+</sup> ≈ Mg<sup>2+</sup> (little or no effect); voltage shift of  $I_{Kr}$  activation: Cd<sup>2+</sup> ≈ Ni<sup>2+</sup> > Co<sup>2+</sup> > Mn<sup>2+</sup> > Ca<sup>2+</sup> ≈ Sr<sup>2+</sup> ≈ Mg<sup>2+</sup> (little or no effect).

show a significant increase in time-dependent current during the voltage step itself, which we have attributed to a voltage shift of inactivation of the transient outward current,  $I_A$ , by Zn<sup>2+</sup>, as has previously been shown (Agus et al., 1991). The results in Fig. 4 A indicate that block of  $I_{Kr}$  occurred without a voltage shift of  $I_{Kr}$  activation. The curve describing the control results in Fig. 4 A corresponds to the Boltzmann equation, with  $V_{1/2} = 12$  mV and  $V_S = 9$  mV.

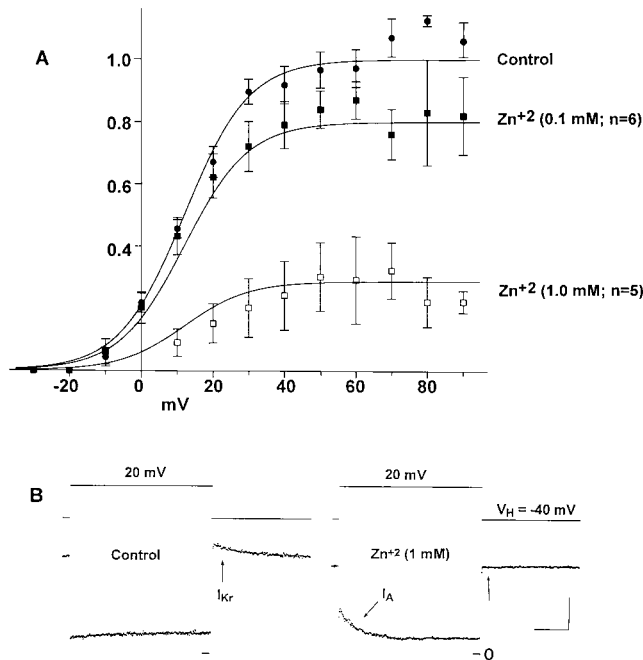


**FIGURE 4** Block of  $I_{Kr}$  by Zn<sup>2+</sup>. (A) Activation curves for  $I_{Kr}$  obtained according to the protocol in Fig. 3 A in the control (●) and in saline containing 0.1 mM Zn<sup>2+</sup> ( $n = 6$ ) (■) and 1 mM Zn<sup>2+</sup> ( $n = 5$ ) (□). All results were normalized by the maximum tail current obtained in control. The curves correspond to  $(1 + \exp(-(V - 12)/9))^{-1} (1 + [Zn^{2+}]/0.4)^{-1}$ , where  $[Zn^{2+}]$  is either 0, 0.1, or 1.0 mM. (B) Records obtained with a step potential to +20 mV in control and with 1 mM Zn<sup>2+</sup>. The tail current in the control (indicated by the arrow) was essentially absent from the test results. We have attributed the significant time-dependent current during the step to +20 mV in the test record to  $I_A$ , as indicated in the Results. Calibrations are 0.5 s and 0.1 nA.

The other two curves in Fig. 4 A are the same as the control, but are scaled by  $(1 + [Zn^{2+}]/K_D)^{-1}$ , with  $K_D = 0.4$  mM. In other words, the  $I_{Kr}$  channel appears to have a binding site on its external surface for Zn<sup>2+</sup> with a dissociation constant of 0.4 mM. The channel is blocked when the site is occupied by Zn<sup>2+</sup>.

Barium (1.0–5.0 mM) has often been used with cardiac preparations to remove  $I_{K1}$  during voltage clamp steps (DiFrancesco, 1981; Brochu et al., 1992), so our expectation was that it would potentially block  $I_{K1}$  in our experiments as well. We did observe significant block of  $I_{K1}$  by Ba<sup>2+</sup> (0.5–2 mM) in steady state. However, the block was time-dependent under these conditions (even in the presence of 1  $\mu$ M E-4031). To our knowledge, similar results have not been reported for cardiac cells, although Standen and Stanfield (1978) observed time-dependent block of  $I_{K1}$  by Ba<sup>2+</sup> in skeletal muscle, and Tang and Yang (1994) reported similar results with Ba<sup>2+</sup> in hIRK2, an inward rectifier channel cloned from human brain that is also found in cardiac tissues.

## DISCUSSION

We have investigated the effects of various divalent cations on  $I_{Kr}$  in a mammalian cardiac ventricular myocyte preparation. Our results concerning the shift of the  $I_{Kr}$  activation curve and the acceleration of the  $I_{Kr}$  channel closing rate are qualitatively similar to the effects of divalent cations on several other preparations, beginning with the original work on this topic by Frankenhaeuser and Hodgkin (1957) on squid giant axons. Those results were originally attributed to a surface charge mechanism, although several reports have demonstrated that this theory, at least in its simplest form, does not account for many of the relevant experimental observations (Gilly and Armstrong, 1982a,b; Armstrong and Cota, 1990). The effects of divalent cations on  $I_{Kr}$  amplitude, specifically our results with Cd<sup>2+</sup>, Ni<sup>2+</sup>, Co<sup>2+</sup>, and Mn<sup>2+</sup>, are qualitatively different from the effects of these ions on channel activation. The observation that Cd<sup>2+</sup> increased  $I_{Kr}$  amplitude significantly more than Ni<sup>2+</sup>, whereas the two ions shifted channel activation by approximately the same amount, further supports the idea that the loci on the  $I_{Kr}$  channel for these two types of effects are different. The effect of Cd<sup>2+</sup> on  $I_{Kr}$  amplitude was originally reported by Follmer et al. (1992) for cat ventricular myocytes. They attributed their result to an interaction between Cd<sup>2+</sup> and the mechanism responsible for inward rectification of the  $I_{Kr}$  channel, which they assumed was either an ion in the cytoplasm, or a membrane-bound, positively charged particle, similar to our original hypothesis concerning  $I_{Kr}$  rectification (Shrier and Clay, 1986). This view requires revision based on the work of Smith et al. (1996) and Spector et al. (1996), who have clearly shown that the apparent rectification of  $I_{Kr}$  is attributable to a very rapid, voltage-gated inactivation mechanism. We have proposed one way in which Cd<sup>2+</sup>, Mn<sup>2+</sup>, Ni<sup>2+</sup>, and Co<sup>2+</sup>

might alter inactivation gating to produce an increase in  $I_{Kr}$  amplitude: a direct interaction between divalent cations and the inactivation gate. Alternatively, the effect could be attributable to a surface charge mechanism, i.e., a voltage shift of the inactivation curve similar to the shift of the activation curve produced by these cations, as shown for  $Cd^{2+}$  in Fig. 3 A. This mechanism appears not to be applicable to our results, as illustrated in Fig. 5 A. The results in Fig. 3 B—the fully activated current-voltage relations in control and in the presence of 5 mM  $Cd^{2+}$ —have been reproduced in Fig. 5 A. The theoretical curve describing the control results in Fig. 5 A is the same as in Fig. 3 B, i.e.,  $I_{Kr} = 0.043(V + 70)/(1 + 6 \exp(0.05V))$  (normalized as described in the Fig. 3 B legend). From this analysis the inferred inactivation curve is given by  $1/(1 + 6 \exp(0.05V))$ , which is shown in Fig. 5 B (solid line). A rightward shift of this curve by 30 mV is illustrated in Fig. 5 B by the dashed line. The current-voltage relation that we would have ob-

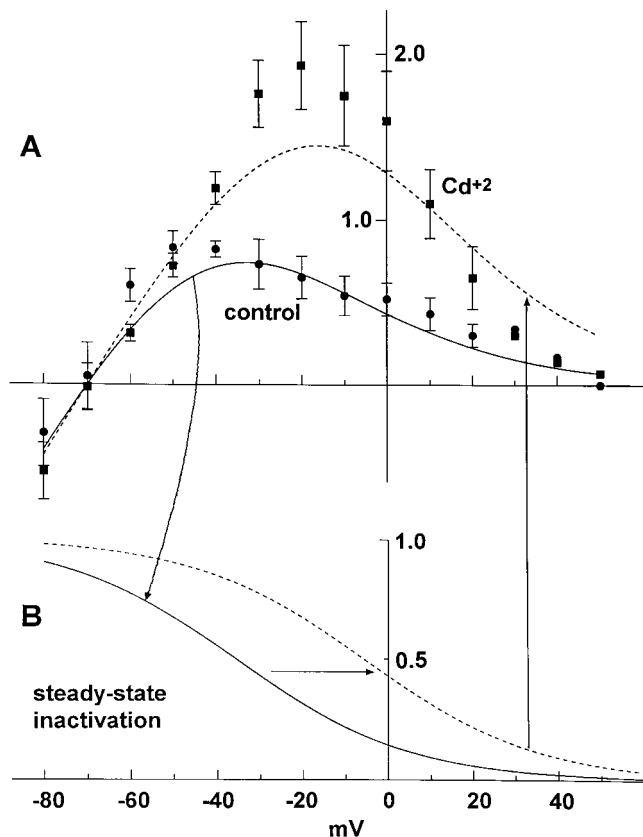


FIGURE 5 Predictions of a simple shift of the  $I_{Kr}$  inactivation for the fully activated  $I_{Kr}$  current-voltage relation. The data in A were taken from Fig. 3 B. The theoretical curve that described the control results is  $0.043(V + 70)/(1 + 6 \exp(0.05V))$ , from which the steady-state inactivation curve can be inferred to be  $(1 + 6 \exp(0.05V))^{-1}$ , shown in B by the solid line. The dashed curve in B illustrates a 30-mV rightward shift of this curve along the voltage axis, i.e.,  $(1 + 6 \exp(0.05(V - 30)))^{-1}$ . The corresponding prediction for the fully activated current-voltage relation is shown in A by the dashed line, i.e.,  $0.043(V + 70)/(1 + 6 \exp(0.05(V - 30)))$ . This curve does not provide a good description of the 5 mM  $Cd^{2+}$  results, as described in the text.

tained in these experiments if this simple shift of inactivation had occurred is shown in Fig. 5 A (dashed line). This prediction deviates significantly from the experimental results. To describe these results, the inactivation curve would have to not only be shifted rightward along the voltage axis, but also steepened considerably, which is effectively what occurs in our model of the  $Cd^{2+}$  results given above (Results). Measurements of inactivation kinetics may help to distinguish between the two mechanisms—a direct interaction between divalent cations and the inactivation gate, or a mechanism more closely related to a surface charge effect.

Our results with  $Co^{2+}$  appear to be inconsistent with the work of Baro and Escande (1989) and Sanguinetti and Jurkiewicz (1991), who found that  $Co^{2+}$  eliminated a small component or “hump” of outward current with a voltage ramp, which the latter authors attributed to block of  $I_{Kr}$ . The analysis in Fig. 6 demonstrates that this result is attributable instead to a voltage shift of the  $I_{Kr}$  activation curve into a voltage range where rectification of its fully activated current-voltage relation is even steeper than in control. We have used our  $Cd^{2+}$  results to illustrate this point. The theoretical description of steady-state activation of  $I_{Kr}$  in control and with 5 mM  $Cd^{2+}$  (Fig. 3 A) is reproduced in Fig. 6 A. Similarly, the fully activated  $I-V$  relations in control and with 5 mM  $Cd^{2+}$  in Fig. 3 B are reproduced in Fig. 6 B. The contribution of  $I_{Kr}$  to net current during a slow voltage ramp is approximately given by its steady-state amplitude, because  $I_{Kr}$  activation is relatively rapid. These results correspond to the product of the steady-state activation and the fully activated  $I-V$  curves, which are given in Fig. 6 C for the control and for 5 mM  $Cd^{2+}$  (curves a and b, respectively). The difference between these results, given in Fig. 6 D, is to be compared with the experimental results for 3 mM  $Co^{2+}$  in figure 2 C of Baro and Escande (1989), and Figure 1 B of Sanguinetti and Jurkiewicz (1991). (Note the block of  $I_{K1}$  by  $Co^{2+}$  in the latter result.) That is, millimolar concentrations of  $Cd^{2+}$  and  $Co^{2+}$  (and  $Mn^{2+}$  and  $Ni^{2+}$ ) reduce outward steady-state current while at the same time increasing peak outward  $I_{Kr}$ . The analysis in Fig. 6 provides a resolution to this paradox. Moreover, it further illustrates that divalent cations do not simply shift the  $I_{Kr}$  inactivation curve along the voltage axis. If this mechanism applied, then the apparent “block” of  $I_{Kr}$  by  $Co^{2+}$  would not have been observed by Sanguinetti and Jurkiewicz (1991). Rather, the difference current from the voltage ramps with 3 mM  $Co^{2+}$  and in control would have been biphasic.

The effects of divalent cations on K channels have been investigated by the use of reducing agents that neutralize the positive charge of the amino group of lysines and histidines, thereby altering the sensitivity of the channel to divalent cations, such as  $Zn^{2+}$  and  $Cd^{2+}$  (Spies and Begenisich, 1994, and references therein). Similar experiments with  $I_{Kr}$  might help to further define the effects of divalent cations on its inactivation gate. Site-directed mutagenesis has been used to localize the amino acid residue where  $Cd^{2+}$  binds to the sodium channel in cardiac and skeletal muscle (Backx et al., 1992). Similar experiments with the HERG K channel

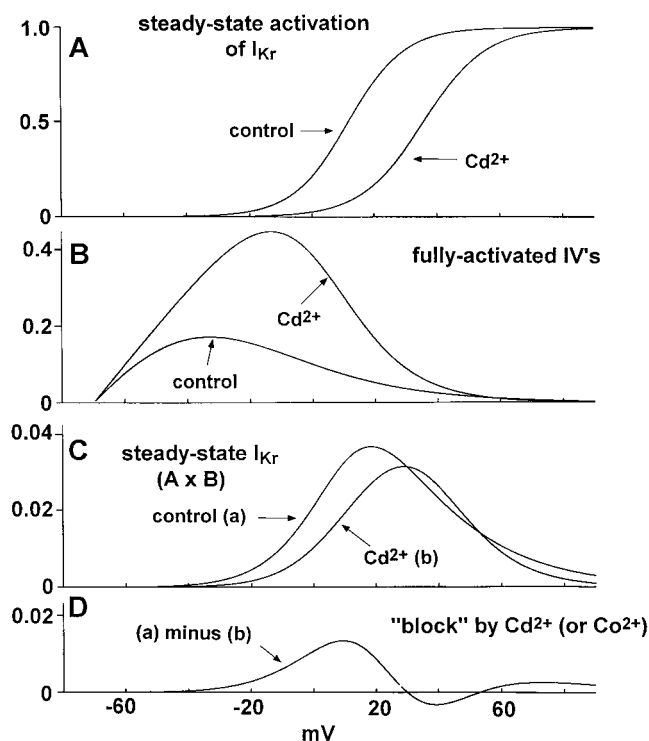


FIGURE 6 Analysis of the apparent "block" of  $I_{Kr}$  by  $Co^{2+}$  during voltage ramps (Baro and Escande, 1989; Sanguinetti and Jurkiewicz, 1991). (A) Theoretical representation of the steady-state activation of  $I_{Kr}$  in control and 5 mM  $Cd^{2+}$  conditions (taken from Fig. 3 A). (Because the effects of  $Co^{2+}$  are quantitatively similar to those of  $Cd^{2+}$ , we have used our  $Cd^{2+}$  results in this analysis.) (B) Fully activated current-voltage relations in control and 5 mM  $Cd^{2+}$  (taken from Fig. 3 B). (C) Steady-state  $I_{Kr}$ . Because of the rapid activation of  $I_{Kr}$ , its contribution to net current during a slow ramp is essentially given by the product of its steady-state activation and fully activated  $I-V$  curves, as shown here. (D) Apparent block of  $I_{Kr}$  during a ramp by  $Cd^{2+}$  (or  $Co^{2+}$ ). The result shown here is the difference between curves a and b in C. This is the current that would be obtained in a full ionic model of the preparation by subtracting the steady-state  $I-V$  curve after the addition of 5 mM  $Cd^{2+}$  to the external solution from the control  $I-V$  curve. That is, an outward current appears to be blocked by  $Cd^{2+}$ , whereas the analysis in A–C demonstrates that this result is attributable to a voltage shift of the activation (A) into a voltage range where the rectification of the fully activated  $I-V$  curve is even steeper than in the control (B).

may help to localize the  $Cd^{2+}$  binding site on its inactivation gate and provide insight into the relative sensitivity of this site for the various different divalent cations.

We gratefully acknowledge excellent technical assistance from Cedric Gordon and Johanne Ouellette. We thank Dr. Betty I. Sasyniuk for helpful discussions during the study.

This work was supported by a grant from the Medical Research Council of Canada (AS). TP was supported by a studentship from MRCC.

## REFERENCES

- Agus, Z. S., I. D. Dukes, and M. Morad. 1991. Divalent cations modulate the transient outward current in rat ventricular myocytes. *Am. J. Physiol.* 261:C310–C318.
- Armstrong, C. M., and G. Cota. 1990. Modification of sodium channel gating by lanthanum. Some effects that cannot be explained by surface charge theory. *J. Gen. Physiol.* 96:1129–1140.
- Armstrong, C. M., and S. R. Taylor. 1980. Interaction of barium ions with potassium channels in squid giant axons. *Biophys. J.* 30:473–488.
- Backx, P. H., D. T. Yue, J. H. Lawrence, E. Marban, and G. F. Tomaselli. 1992. Molecular localization of an ion-binding site within the pore of mammalian sodium channels. *Science*. 257:248–251.
- Baro, I., and D. Escande. 1989. A long lasting  $Ca^{2+}$ -activated outward current in guinea-pig atrial myocytes. *Pflugers Arch.* 415:63–71.
- Brochu, R. M., J. R. Clay, and A. Shrier. 1992. Pacemaker current in single cells and in aggregates of cells dissociated from the embryonic chick heart. *J. Physiol. (Lond.)*. 454:503–515.
- Carmeliet, E. 1993. Use-dependent block and use-dependent unblock of delayed rectifier  $K^+$  current by amokalant in rabbit ventricular myocytes. *Circ. Res.* 73:857–868.
- Clay, J. R. 1995. Asymmetric modulation and blockade of the delayed rectifier in squid giant axons by divalent cations. *Biophys. J.* 69:1773–1779.
- Clay, J. R., A. Ogbaghebril, T. Paquette, B. I. Sasyniuk, and A. Shrier. 1995. A quantitative description of the E-4031 sensitive repolarization current in rabbit ventricular myocytes. *Biophys. J.* 69:1830–1837.
- Daleau, P., M. Khalifa, and J. Turgeon. 1997. Effects of cadmium and nisoldipine on the delayed rectifier potassium current in guinea pig ventricular myocytes. *J. Pharmacol. Exp. Ther.* 281:826–833.
- DiFrancesco, D. 1981. A study of the ionic nature of the pace-maker current in calf Purkinje fibers. *J. Physiol. (Lond.)*. 314:377–393.
- Eaton, D. C., and M. S. Brodwick. 1980. Effects of barium on the potassium conductance of squid axon. *J. Gen. Physiol.* 75:727–750.
- Ficker, E., M. Tagliatela, B. A. Wible, C. M. Henley, and A. M. Brown. 1994. Spermine and spermidine as gating molecules for inward rectifier  $K^+$  channels. *Science*. 266:1068–1072.
- Follmer, C. H., N. J. Lodge, C. A. Cullinan, and T. J. Colatsky. 1992. Modulation of the delayed rectifier,  $I_{Kr}$ , by cadmium in cat ventricular myocytes. *Am. J. Physiol.* 262:C75–C83.
- Frankenhaeuser, B., and A. L. Hodgkin. 1957. The action of calcium on potassium conductance of squid axons. *J. Physiol. (Lond.)*. 137:218–244.
- Giles, W. R., and Y. Imaizumi. 1988. Comparison of potassium currents in rabbit atrial and ventricular cells. *J. Physiol. (Lond.)*. 405:123–145.
- Gilly, W. F., and C. M. Armstrong. 1982a. Slowing of sodium channel opening kinetics in squid axon by extracellular zinc. *J. Gen. Physiol.* 79:935–964.
- Gilly, W. F., and C. M. Armstrong. 1982b. Divalent cations and the activation kinetics of potassium channels in squid giant axon. *J. Gen. Physiol.* 79:965–996.
- Hille, B. 1992. *Ionic Channels of Excitable Membranes*, 2nd ed. Sinauer Associates, Sunderland, MA. 457–471.
- Isenberg, G., and U. Klockner. 1982. Calcium tolerant ventricular myocytes prepared by preincubation in a "KB medium." *Pflugers Arch.* 395:6–18.
- Matsuda, H., A. Saigua, and H. Irisawa. 1987. Ohmic conductance through the inwardly rectifying K channel and blocking by internal  $Mg^{2+}$ . *Nature*. 325:156–159.
- Mitra, R., and M. Morad. 1985. A uniform enzymatic method for dissociation of myocytes from hearts and stomachs of vertebrates. *Am. J. Physiol.* 249:H1056–H1060.
- Noble, D., and R. W. Tsien. 1969. Outward membrane currents activated in the plateau range of potentials in cardiac Purkinje fibers. *J. Physiol. (Lond.)*. 200:205–231.
- Ogbaghebril, A., and A. Shrier. 1994. Inhibition of metabolism abolishes transient outward current in rabbit atrial myocytes. *Am. J. Physiol.* 266:H182–H190.
- Sanguinetti, M. C., and N. K. Jurkiewicz. 1990a. Two components of cardiac delayed rectifier  $K^+$  current: different sensitivity to block by class III antiarrhythmic agents. *J. Gen. Physiol.* 96:195–215.
- Sanguinetti, M. C., and N. K. Jurkiewicz. 1990b. Lanthanum blocks a specific component of  $I_{Kr}$  and screens membrane surface charge in cardiac cells. *Am. J. Physiol.* 259:H1881–H1889.

- Sanguinetti, M. C., and N. K. Jurkiewicz. 1991. Delayed rectifier outward  $K^+$  current is composed of two currents in guinea pig atrial cells. *Am. J. Physiol.* 260:H393–H399.
- Shimoni, Y., R. B. Clark, and W. R. Giles. 1992. Role of an inwardly rectifying potassium current in rabbit ventricular action potential. *J. Physiol. (Lond.)* 448:709–727.
- Shioya, T., H. Matsuda, and A. Noma. 1993. Fast and slow blockade of the inward-rectifier  $K^+$  channel by external divalent cations in guinea-pig cardiac myocytes. *Pflugers Arch.* 422:427–435.
- Shrier, A., and J. R. Clay. 1986. Repolarization currents in embryonic chick atrial heart cell aggregates. *Biophys. J.* 50:861–874.
- Smith, P. L., T. Baukowitz, and G. Yellen. 1996. The inward rectification mechanism of the HERG cardiac potassium channel. *Nature.* 379: 833–836.
- Spector, P. S., M. E. Curran, A. Zou, M. T. Keating, and M. C. Sanguinetti. 1996. Fast inactivation causes rectification of the  $I_{Kr}$  channel. *J. Gen. Physiol.* 107:611–619.
- Spires, S., and T. Begenisich. 1994. Modulation of potassium channel gating by external divalent cations. *J. Gen. Physiol.* 104:675–692.
- Standen, N. B., and P. R. Stanfield. 1978. A potential- and time-dependent blockade of inward rectification in frog skeletal muscle fibers by barium and strontium ions. *J. Physiol. (Lond.)* 280:169–191.
- Tang, W., and X. C. Yang. 1994. Cloning a novel human brain inward rectifier potassium channel and its functional expression in *Xenopus* oocytes. *FEBS Lett.* 348:239–243.
- Vandenberg, C. A. 1987. Inward rectification of a potassium channel in cardiac ventricular cells depends on internal magnesium ions. *Proc. Natl. Acad. Sci. USA.* 84:2560–2564.